



ELSEVIER

Available online at [www.sciencedirect.com](http://www.sciencedirect.com)

 ScienceDirect

Energy Procedia 4 (2011) 637–644

**Energy  
Procedia**

[www.elsevier.com/locate/procedia](http://www.elsevier.com/locate/procedia)

GHGT-10

## Oxygen production technologies for IGCC power plants with CO<sub>2</sub> capture

Jacopo Tonziello, Michela Vellini\*

*Department of Industrial Engineering, University of Rome "Tor Vergata", Via del Politecnico 1 - 00133 Rome, Italy*

---

### Abstract

IGCC power plants seem to represent one of the most appealing options to produce electric energy from coal and low grade solid fuels with interesting plant efficiency and low environmental impact. As a matter of fact the majority of gasification-based power plants are equipped with oxygen-blown gasifiers which have two main advantages with respect to air-blown reactors: high values of cold gas efficiency and an N<sub>2</sub> deprived syngas. The aim of this paper is to compare two different oxygen production technologies for oxidant supply to the gasification island. An IGCC power plant with pre-combustion CO<sub>2</sub> capture has been modelled considering: (i) a cryogenic distillation ASU based on a pumped liquid oxygen cycle; (ii) an innovative OTM-based oxygen production technology integrated in the power island. An overall heat and material balance has been estimated to evaluate plant performances and compare the two options; our thermodynamic analysis shows a promising improvement of the overall plant performance for the OTM-based IGCC nonetheless several key issues deserve a more in depth analysis to assess the real potentialities of membrane-based oxygen production technology.

© 2011 Published by Elsevier Ltd. Open access under [CC BY-NC-ND license](http://creativecommons.org/licenses/by-nc-nd/3.0/).

*Keywords:* ASU; OTM; IGCC; Carbon Capture and Storage.

---

### 1. Introduction

Despite concerns about rising concentrations of greenhouse gases in the atmosphere, fossil fuels are likely to play a major role in the energetic scenario of the medium term future. Among fossil fuels, coal is abundant, has a wide geographic distribution and can be considered relatively cheap. However, carbon dioxide produced as a result of fossil fuel combustion is the main responsible of human-induced climate change. During the last century, the concentration of CO<sub>2</sub> in the atmosphere increased from 275 to 387 ppm producing, according to the majority of scientific community, measurable increases in global temperatures. Climate models indicate that continuation of this trend will dramatically change the global climate by 2100. The so called "clean coal technologies" represent a real option to mitigate CO<sub>2</sub> emissions from power plants, in particular coal-fired power plants have been extensively studied in the last fifteen years and many researchers have proposed different plant configurations for CO<sub>2</sub> capture. These schemes are generally based on three different strategies: (i) pre-combustion of fuel, in this option the heating value of the fossil fuel is relocated to hydrogen and carbon dioxide is removed before combustion from a high pressure stream by means of physical absorption processes or membrane reactors [1,2]; (ii) post-combustion separation

of CO<sub>2</sub> from exhaust gases with absorption or adsorption processes [3]; (iii) oxygen combustion, whose products mainly consist of CO<sub>2</sub> and water, the latter easily removed by condensation [4]. In this paper we have focused our attention to the first option applied to coal gasification; the core of the process is an oxygen-blown gasifier which requires, according to the reactor size, an elevated oxygen production capacity. At present only cryogenic air separation can be used for large-scale oxygen production; in this process the inlet air must be filtered, compressed and chilled to about -180°C, this stream is then distilled in large columns to separate air into its components, based on differences in their boiling points. Cryogenic ASUs produce oxygen with purity greater than 99% mol. with plant size up to 150000 m<sup>3</sup><sub>n</sub>/h [5]. This technology, nowadays mature, has been under development for about a century but it still requires large energy consumptions and high investment costs. An advancement in air separation technologies has been recently proposed by major chemical industries and is based on oxygen transport membranes (OTM). In this process an oxygen partial pressure differential imposed across a ceramic membrane at high temperature drives oxygen ions from the high partial pressure side to the low partial pressure side. Oxygen permeation through ceramic compounds has been extensively studied in the last thirty years after the pioneering work of Teraoka et al. [6] on mixed conduction perovskites and in the last ten years Air Products has been developing ion transport membrane technology with U.S. Dept. of Energy (DOE) support [7,8]. The process is 100% selective to oxygen transport and creates very little pressure loss in the feed air stream. This enables compact, low-cost devices that have both lower capital and compression-energy requirements compared to cryogenic ASUs [7,8].

However, unlike cryogenic ASUs, membrane-based air separation units do not produce a pure stream of nitrogen as a by-product (even with an infinitely large membrane area, a fraction of oxygen would remain in the retentate stream). An inert gas, such as nitrogen is used in IGCC power plants for NO<sub>x</sub> abatement in the gas turbine combustor. In fact, when a large size, heavy duty gas turbine designed to run on natural gas switches to a hydrogen rich syngas, the stoichiometric flame temperature has to be kept below 2300 K to reduce thermal NO<sub>x</sub> formation [9]. To overcome this problem we propose a plant configuration with two OTMs in series: the first membrane is devoted to oxygen separation for gasifier feeding while the second one provides a further purification step in which a fraction of the retentate stream from the first membrane is deprived of oxygen to obtain an high purity N<sub>2</sub> stream that is injected in the gas turbine combustor for syngas dilution.

## 2. Large-scale oxygen production technologies

In the following paragraphs we provide a brief description of the two oxygen production technologies integrated in the gasification-based power plants.

### *Cryogenic air separation units*

In this paper we refer to a liquid oxygen cycle in which oxygen is pumped to the gasifier operating condition in liquid phase, avoiding the installation of the oxygen compressor that represent a high-cost, critical component. In order to assure easier start-up and higher flexibility we have considered a stand-alone ASU without gas turbine integration. Air separation is performed in four main steps: air compression, purification, heat recovery and distillation. More in detail, as shown in Fig.1, ambient air is filtered and compressed to 5.7 bar in a multi-stage ( $\beta_{st} \sim 2$ ) inter-cooled compressor; subsequently it is cooled first with cooling water and then in a direct contact cooler (up to 20°C). This cooling reduces the moisture content of the saturated air, thus reducing the expenditure for the H<sub>2</sub>O removal in the zeolite adsorbers. In the purification section, water vapour and carbon dioxide are removed in the molesieve together with the less volatile hydrocarbons such that during the ensuing cooling in the heat exchanger to about 100 K, no ice or CO<sub>2</sub>-snow is formed by desublimation (this would gradually block the heat exchanger). The more volatile hydrocarbons accumulate in the bath of the main evaporator and are removed with the liquid oxygen. This is important for the safety of the air separation unit because their concentration must remain far below the solubility and explosion limit. The cooled, purified air is sent to the main heat exchanger in the cold-box; a fraction of this air is further compressed and liquefied in the heat exchanger thus enabling the so-called “internal compression” of the oxygen: the released condensation heat vaporizes the liquid compressed oxygen (with a purity of 95% mol.) which is compressed to the gasifier operating conditions by a cryogenic pump. The liquefied high-pressure air is expanded into the low pressure column at a suitable tray via a throttle valve. In the pressure column the gaseous and liquid air is pre-separated and the rectification is crucially determined by the volatilities of the components, which goes hand in hand with their boiling temperatures. Nitrogen, which is more volatile, accumulates at the top of the pressure column. At the bottom of the column an oxygen-enriched liquid with an O<sub>2</sub> content of ~ 40% is formed. In

the low-pressure column operated at about 1.3 bar, the final separation into pure oxygen as sump product, pure nitrogen as top product and residual gas withdrawn from an intermediate stage, takes place. The gaseous nitrogen at the top of the pressure column is liquefied in the main condenser. This condenser is cooled by evaporating liquid oxygen from the sump of the low-pressure column. Condenser and evaporator are designed as a coupled heat transfer unit: part of the condensate serves as reflux for the high pressure column, the rest is expanded and fed as reflux to the top of the low-pressure column. Nitrogen for NO<sub>x</sub> abatement is extracted from the top of the low pressure column, compressed and injected in the gas turbine combustor. A detailed analysis of advanced cryogenic ASUs and their integration in IGCC power plants can be found in [10].

### Oxygen transport membranes

OTM are non-porous, mixed ion and electron-conducting materials operating typically at high temperatures. Membrane performance strongly depends on the properties of its materials, which are mainly governed by the material compositions and structures. Materials suited for OTM application typically are perovskites (ABO<sub>3-δ</sub> and A<sub>2</sub>BO<sub>4±δ</sub>), fluorites (A<sub>δ</sub>B<sub>1-δ</sub>O<sub>2-δ</sub> and A<sub>2δ</sub>B<sub>2-2δ</sub>O<sub>3</sub>) or dual phases by the introduction of metal or ceramic elements (A and B are different cations which can be representative of a number of elements). If an oxygen transport membrane is placed under an oxygen chemical potential gradient, oxygen anions permeate from the high oxygen chemical potential side to the low oxygen chemical potential side while overall charge neutrality is maintained by a counterbalancing flux of electrons. Temperature is one of the parameters that mainly influence permeance and, provided that the process is thermally activated, it is typically carried out in the temperature range of 800-900°C and between 10-30 bar on the feed side and low to sub-atmospheric pressure on the permeate side.

The transport of oxygen across the membrane typically occurs in five different steps [11]: (i) mass transfer of gaseous O<sub>2</sub> from the gas stream to the membrane surface (*high-pressure side*), (ii) adsorption of O<sub>2</sub> molecules followed by dissociation into ions and incorporation into bulk (*surface reaction*), (iii) transport of oxygen ions through the membrane (*bulk diffusion*), (iv) association of oxygen ions followed by desorption of oxygen molecules (*surface reaction*), (v) mass transfer of O<sub>2</sub> from the membrane surface to the gas stream (*low-pressure side*). Compared to other steps, steps (i) and (v) are simpler mass transport processes and the gas-phase resistance can be considered negligible. Surface reactions from step (ii) and (iv) and bulk diffusion from step (iii) are more important processes. The slowest process is expected to limit the overall rate of oxygen permeation [11,12]; when the diffusion process can be considered the slowest step the oxygen flux can be described by the Wagner law [7,8]:

$$j_{O_2} = \frac{RT}{4n^2 F^2 L} \left( \frac{\sigma_e \sigma_i}{\sigma_e + \sigma_i} \right) \ln \left( \frac{p_{O_2,f}}{p_{O_2,p}} \right) \quad (1)$$

where  $j_{O_2}$  is the local oxygen flux [mol/(s·m<sup>2</sup>)],  $F$  is the Faraday's constant [C/mol],  $R$  is the ideal gas constant [J/(mol·K)],  $T$  is the absolute temperature [K],  $n$  is the charge of the charge carrier (for oxygen  $n=2$ ),  $L$  is the membrane thickness [m],  $\sigma_i$  and  $\sigma_e$  are the ionic and electronic conductivity respectively [S/m],  $p_{O_2,f}$  and  $p_{O_2,p}$  are the oxygen partial pressures at the feed and at the permeate sides [bar]. A simplification can be introduced for some compounds (such as in perovskite-based) in which electronic conductivity is much higher than the ionic conductivity ( $\sigma_e \gg \sigma_i$ ), in these cases the Wagner equation can be rewritten as:

$$j_{O_2} = \frac{RT \sigma_i}{16 F^2 L} \ln \left( \frac{p_{O_2,f}}{p_{O_2,p}} \right) \quad (2)$$

This expression identifies the natural logarithm of the oxygen partial pressure ratio as the driving force for the oxygen flux. Usually the values of  $\sigma_i$  and  $L$  depend on the material and  $T$  is fixed by the membrane operating conditions, consequently membrane surface can be limited increasing oxygen partial pressure ratio. This can be achieved with: (i) high absolute pressure ratio across the membrane which can be achieved with a strong air compression of the feed stream, (ii) an high flow of sweep gas on the permeate side in order to dilute the oxygen stream.

In our membrane model, described in detail elsewhere [13], we have assumed bulk diffusion as the limiting step, according to the work of Ito et al. [14]. They developed a new mixed conducting oxide (SrCo<sub>0.9</sub>Nb<sub>0.1</sub>O<sub>3-δ</sub>) and tested several membrane tubes with a dense membrane of 50 μm and a porous layer of 5 μm under high pressure air fluxes

(from 10 atm to 20 atm) at 850°C and 900°C. The oxygen permeation rate measured follows the Wagner law suggesting that the porous layer acts both as a support for the membrane against large pressure differences and as a promoter for the surface reactions as well as the active layer on the membrane. The ionic conductivity was estimated using the Wagner law and the measured permeation rate, a value of 100 S/m was found at 900°C and 80 S/m at 850°C.

As a final remark we briefly point out that an OTM-based air separation unit can be designed with different module configurations, such as: tube and plate, single tube, multi-channel monolith and hollow fibers. Each concept has advantages and disadvantages in reachable surface area per unit volume ( $\text{m}^2/\text{m}^3$ ), sealing technology and tolerance to a sweep gas on the permeate side. In the following we have assumed a counter-current, sweep flow configuration without defining a detailed module geometry but simply evaluating membrane area as an output of our one-dimensional model. An exhaustive analysis on membrane module design can be found in a recent paper of Vente et al. [15].

### 3. IGCC power plants with CO<sub>2</sub> capture

To assess the thermodynamic performance of the two options proposed, a comprehensive IGCC simulation has been set up. Heat and material balances have been evaluated with different commercial softwares: the gasification island has been simulated with Aspen Plus<sup>TM</sup>, the power island with GateCycle<sup>TM</sup> while a one-dimensional membrane module has been set up ad hoc in Matlab<sup>TM</sup>. In the following we provide a brief description of the plant layouts proposed in Fig.1 and Fig.2. The main technical assumptions adopted through the calculations are reported in the Appendix.

#### *Conventional IGCC with pre-combustion CO<sub>2</sub> capture*

In this paper we have considered an IGCC power plant equipped with an oxygen-blown, entrained-flow, slurry-feed gasifier. Coal (Illinois#6, LHV=24,8 MJ/kg) is mixed with water and the resulting slurry (63% wt. solids) is heated and fed to the gasifier with an oxidant stream produced by the cryogenic air separation unit. Gasification pressure is set at 70 bar and the temperature of 1330°C is achieved varying the mass flow of the oxidant feed. The high operating temperature enables to model the reactor at chemical equilibrium with reasonable accuracy. Carbon conversion of the gasifier is assumed to be 99.5% and heat losses are fixed at 0,5% of the LHV thermal input. The raw syngas and the molten slag exit the gasifier and are quenched by direct contact with a preheated water stream so that syngas is fully saturated and scrubbed for ash and soluble compounds removal. The stream is then sent to the water gas shift reactors where CO and H<sub>2</sub>O are converted to H<sub>2</sub> and CO<sub>2</sub> through the following exothermic reaction:  $\text{CO} + \text{H}_2\text{O} \leftrightarrow \text{CO}_2 + \text{H}_2$  ( $\Delta h = 41.2$  kJ/mol). We have assumed a sulphur tolerant CoMo catalyst (sour shift catalyst) capable of bringing the whole gas mixture to equilibrium. The shift reaction is performed in two reactors in series: the first works at high temperature (350-450°C) and accomplishes much of the CO conversion, the second one - at lower temperature (200-250°C) - brings the CO concentration down to a few percent by volume. Syngas from the quench chamber is saturated with water thus satisfying the steam requirement of shift reactors that is significantly larger than stoichiometrically required for the CO conversion. This is attributable to catalyst stability requirements concerning the minimum inlet steam/CO-ratio and the maximum operating temperature, as well as to enhance the equilibrium conversion. Between the two stages and during shift reactions heat recovery is performed by a network of heat exchangers, producing: (i) intermediate pressure steam (vaporization and superheating), (ii) warm water for slurry and quench make-up, (iii) hot water for syngas saturation. The syngas, exiting the shift reactors section is cooled to very low temperature (about 35°C) with water condensation and finally purified to remove H<sub>2</sub>S and CO<sub>2</sub>. Since the gasifier is pressurized at 70 bar, the high CO<sub>2</sub> partial pressure in the stream favours a physical absorption process like the two stage Selexol process in which dimethyl ether of polyethylene glycol is used as a solvent. Selexol process datas are proprietary and not available in the open literature so a detailed simulation of the purification section is out of the scope of this work. We have assumed the energy requirements and product streams purities of this section as calculated in [16] and reported in [3]. The CO<sub>2</sub> stream separated from the syngas is compressed up to 150 bar and a final cooling makes it available at the plant boundaries in liquid phase. After the purification step, syngas is moisturized in a saturator, heated, passed through an expander for shaft work recovery and burned in the gas turbine with nitrogen for NO<sub>x</sub> abatement. Heat from the flue gases of the gas turbine is recovered in a three pressure level heat recovery steam generator coupled with a steam turbine with water condensation.

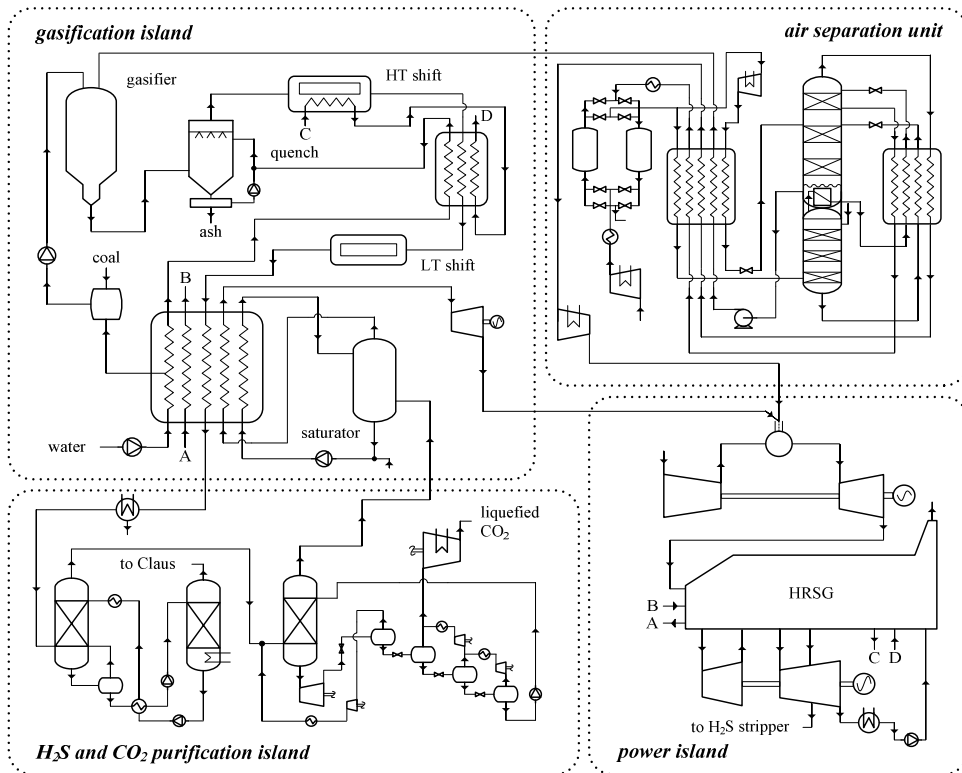


**Figure 1** - Detailed plant configuration of an IGCC power plant with cryogenic ASU and CO<sub>2</sub> capture.

#### Oxygen transport membrane-based IGCC with pre-combustion CO<sub>2</sub> capture

The IGCC power plant equipped with OTM is shown in Fig.2. The gasification island has the same plant layout of the previous configuration while the power island and the oxygen production section are now integrated. The fraction of the compressed air required by the OTM is extracted from the main air compressor of the gas turbine and an additional combustion chamber is provided to set air temperature to the membrane operating conditions; the hot depleted air is mixed with the main air stream, burned in the combustion chamber and then expanded for shaft work conversion. The boost compressor offsets the pressure losses in the new circuit ( $\Delta p_{rec} + \Delta p_{cc,aux} + \Delta p_{OTM}$ ) while the internal recuperator lower the fuel input in the auxiliary combustion chamber. The syngas burnt in the gas turbine has an hydrogen fraction of ~90% mol. thus requiring an inert gas dilution in the combustor after the saturation step. To provide N<sub>2</sub>, the retentate stream of the first membrane has to be purified to lower the oxygen molar fraction to about 1% mol. (a suitable value for NO<sub>x</sub> abatement [17]). In the plant layout of Fig.2 a fraction of the retentate stream from the first membrane (M1) enters the second membrane (M2) as feed stream while the other fraction of the retentate goes in the main combustor. Oxygen permeated through M1 and M2 is separated from steam by condensation after a heat recovery section. The temperature fixed in the final flash set the oxygen stream purity: we have imposed 30°C thus obtaining a stream with about 97.5% mol. O<sub>2</sub>. Oxygen is then compressed to the gasifier operating conditions and the traces of water are removed in knockout drums during intercooling thus leaving an almost pure oxygen stream (99.7% mol.). Water separated in the flash drum is mixed with a make-up stream and then superheated up to 750°C before being used as sweep gas in the OTM. The use of a sweep gas lowers the oxygen concentration on the permeate side and enhance the oxygen partial pressure ratio across the membrane thus increasing the oxygen recovery for a given membrane area.

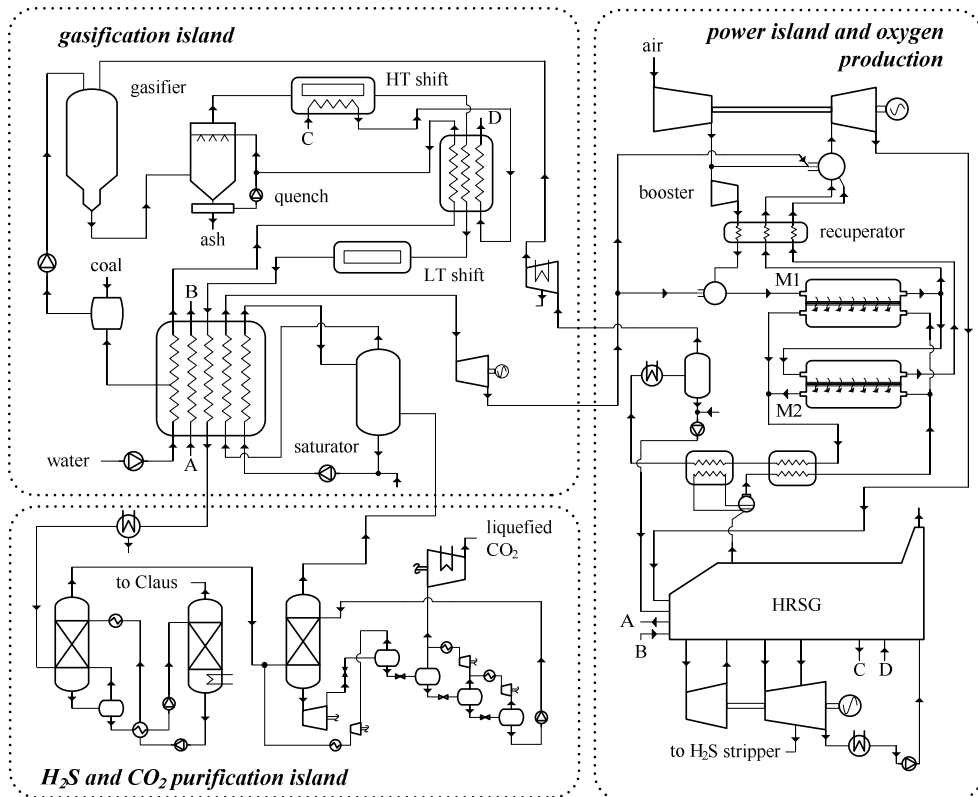


**Figure 2** - Detailed plant configuration of an IGCC power plant with OTM and CO<sub>2</sub> capture.

The second membrane performs a purification step of an oxygen-depleted stream ( $\sim 8\%$  mol. O<sub>2</sub>) thus requiring a sweep flow to drive efficiently the oxygen flux. Fig.3 shows the effect of sweep flow on membrane area: the vertical line identifies the minimum sweep flow required to perform the separation while the horizontal line represent the first membrane area, taken as reference. We have imposed arbitrarily a relative membrane area ( $A_2/A_1$ ) of 0.33 thus requiring a sweep flow of 6% with respect to the feed flow (molar basis).

#### 4. Results and discussion

The thermodynamic performances of the two reference configurations are reported in Tab.1. We have assumed a thermal input in the gasifier of 800 MW<sub>th</sub> (LHV basis). As shown in Tab.1 the main differences from a thermodynamic point of view rely in the power cycle performance and the auxiliary components (compressors) energy requirements. The gasification island shows the same energy requirements in both plant configurations, the

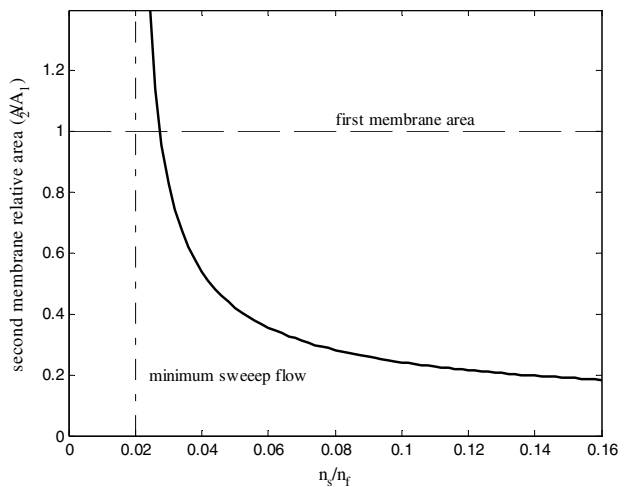


**Figure 3** - Sweep flow effect on second membrane (M2) area.

main difference in the process is the oxidant stream fed to the gasifier. The cryogenic ASU produces a stream of O<sub>2</sub> compressed in a liquid cycle delivered at ambient temperature with a purity of 95% mol. while the OTM produces an almost pure oxygen stream (99.7% mol.) that is compressed in an intercooled compressor and enters the gasifier at about 200°C. As a result the oxidant mass flow required by the gasifier fed by the cryogenic ASU is higher because the stream is cold (17°C) and has a lower purity. Finally the syngas exiting the gasifier has a lower LHV and a higher mass flow.

The energy requirements for oxygen production and nitrogen compression are 54.5 MW for the cryogenic-based ASU while the configuration based on OTM has 13.3 MW for oxygen compression and 6.9 MW for the booster air compressor. The gas turbine shows a performance decrease in the OTM-based cycle because a fraction of the syngas is burnt in the auxiliary combustor.

As a final result the net electric power of the OTM-based configuration increases of 2.9% with respect to the cryogenic-based option and the net LHV efficiency increases of 1.05 percentage point.

## 5. Conclusions

Oxygen production is a critical point for IGCC power plants, cryogenic air distillation is a mature technology that has been under development for about a century but it still requires large energy consumptions and high investment costs. In this paper we have proposed an OTM-based IGCC with pre-combustion CO<sub>2</sub> capture, the oxygen production unit is integrated with the gas turbine and two membrane stages in series have been adopted for oxygen and nitrogen separation. A full plant heat and mass balance has shown a promising improvement of the overall plant performance compared to an IGCC equipped with pre-combustion CO<sub>2</sub> capture and a pumped liquid oxygen cryogenic ASU. The plant global efficiency has increased of about 1 percentage point and the specific power output of 2.9%. A full plant optimization requires a deep knowledge of the costs of components not industrially available today, while the aim of the present paper was devoted to assess the thermodynamic potential of the OTM technology coupled with IGCC power plants and CO<sub>2</sub> capture. The overall performances of the OTM-based power plant seem very interesting and justify the research efforts of the gas processing leading companies; further work should be carried out to identify the optimal strategy for the OTM-GT integration, the membrane module configuration and operating conditions (operating pressure, sweep flow).

## References

1. Chiesa P., Consonni S., “Shift Reactors and Physical Absorption for Low-CO<sub>2</sub> Emission IGCCs”, *Journal of Engineering for Gas Turbines and Power*, 121 (1999), pp. 295-305.
2. Chiesa P., Kreutz T., Lozza G. “CO<sub>2</sub> Sequestration from IGCC Power Plants by Means of Metallic Membranes”, *Journal of Engineering for Gas Turbines and Power*, 129 (2007), pp. 123-134.
3. Romano M., “Advanced Coal-Fired Power Plants with CO<sub>2</sub> Capture”; PhD thesis, Politecnico di Milano, Italy; 2008.
4. Pelliccia G., “Decarbonized Electricity Production from the Oxycombustion of Coal and Heavy Oils”, PhD thesis, Politecnico di Milano, Italy 2004.
5. Berger M., Meilinger M., Schwenk D., Wilde K., The Air Gases Nitrogen, Oxygen and Argon, in H.W. Häring (ed.), “Industrial Gases Processing”, chap. 2, Wiley, 2008.
6. Teraoka Y., Zhang H.M., Yamazoe N., “Oxygen-Sorptive Properties of Defect Perovskite-Type La<sub>1-x</sub>Sr<sub>x</sub>Co<sub>1-y</sub>Fe<sub>y</sub>O<sub>3-δ</sub>”, *Chemistry Letters* 9 (1985a), pp.1367-1370.

**Table 1** - Thermodynamic performances of the IGCC power plants with pre-combustion CO<sub>2</sub> capture considered in this study.

	IGCC <sub>Cryo-ASU</sub>	IGCC <sub>OTM</sub>
<i>Electric power (MW<sub>e</sub>)</i>		
Coal handling, milling and slurry pumps	-1.7	-1.7
Slag handling	-0.6	-0.6
Gasification island process pumps	-1.1	-1.1
Air separation unit	-33.9	-
N <sub>2</sub> compressor	-20.6	-
O <sub>2</sub> compressor	-	-13.3
Syngas expander	7.9	7.9
Selexol plant auxiliaries	-8.3	-8.3
CO <sub>2</sub> compressors	-15.1	-15.1
Gas turbine	244.5	216.7
Booster compressor	-	-6.9
Steam cycle	117.3	119.1
<i>Overall performance</i>		
Heat input, LHV (MW <sub>th</sub> )	800.0	800.0
Net electric power (MW <sub>e</sub> )	288.5	296.9
Net LHV efficiency (%)	36.07	37.12

7. Dyer P., Richards R., Russek S., Taylor D., “Ion Transport Membrane Technology for Oxygen Separation and Syngas Production”, *Solid State Ionics* 134 (2000), pp.21-33.
8. A. Bose (ed.), “Inorganic Membranes for Energy and Environmental Applications”, Springer 2009.
9. Chiesa P., Lozza G., “Using hydrogen as gas turbine fuel”, *Journal of Engineering for Gas Turbines and Power*, 127 (2005), pp. 73-80.
10. Tonziello J., Vellini M., “Cryogenic Air Separation Units Simulation and Integration with IGCC Power Plants”, proc. of 64<sup>th</sup> ATI National Conference, Aquila-Montesilvano, Italy, 8-11 September 2009 (in italian).
11. Leo A., Liu S., Diniz da Costa J. C., “Development of Mixed Conducting Membranes for Clean Coal Energy Delivery”, *International Journal of Greenhouse Gas Control* 3 (2009), pp.357-367.
12. Sunarso J., Baumann S., Serra J. M., Meulenber W.A., Liu S., Lin Y.S., Diniz da Costa J.C., “Mixed Ionic–Electronic Conducting (MIEC) Ceramic-Based Membranes for oxygen separation”, *Journal of Membrane Science* 320 (2008), pp.13-41.
13. Manno M., Tonziello J., Vellini M., “Oxygen Transport Membranes for Gasification-based Power Plants. Part A: Current Technology and Membrane Model Description”, proc. of 65<sup>th</sup> ATI National Conference, Chia Laguna (CA), Italy, 13-17 September 2010.
14. Ito W., Nagai T., Sakon T., “Oxygen Separation from Compressed Air Using a Mixed Conducting Perovskite-Type Oxide Membrane”, *Solid State Ionic* 178 (2007), pp.809-816.
15. Vente J., Haije W., IJpelaan R., Rusting F., “On the Full-Scale Module Design of an Air Separation Unit Using Mixed Ionic Electronic Conducting Membranes”, *Journal of Membrane Science* 278 (2006), pp.66-71.
16. NETL: “Cost and Performance Baseline for Fossil Energy Plants”; 2007. [www.netl.doe.gov/energy-analyses/pubs/Bituminous%20Baseline\\_Final%20Report.pdf](http://www.netl.doe.gov/energy-analyses/pubs/Bituminous%20Baseline_Final%20Report.pdf).
17. Allam R., “Improved Oxygen Production Technologies”, *Energy Procedia* 1 (2009), pp.461-470.

## Appendix

The following table details the main assumptions adopted for the plants performance evaluation.

<i>Gasifier</i>		<i>Shift reactors</i>	
Coal - Illinois #6		Pressure losses in each reactor (%)	2
Gasification pressure (bar)	70	First reactor outlet temperature (°C)	400
Gasification temperature (°C)	1330	Second reactor inlet temperature (°C)	230
Slurry concentration (% wt. )	63		
Carbon conversion (%)	99.5	<i>Oxygen compressor</i>	
Heat losses (% LHV coal)	0.5	Pressure of delivered oxygen (bar)	84
		Oxygen compressor polytropic efficiency (%)	82
		Compressor electrical/mechanical efficiency (%)	94
<i>Cryogenic ASU</i>		<i>Physical absorption and CO<sub>2</sub> compression</i>	
Main air compressor delivery pressure (bar)	5.7	Temperature of absorption column (°C)	35
Number of intercoolers	3	Fraction of CO <sub>2</sub> removed to sequestration (%wt.)	95
Intercoolers pressure losses (%)	1	Fraction of H <sub>2</sub> S removed (%wt.)	100
Air compressor polytropic efficiency (%)	85	CO <sub>2</sub> to Claus plant (kg <sub>CO2</sub> /kg <sub>H2S</sub> )	1.46
Cryogenic pump isentropic efficiency (%)	75	Auxiliaries consumption of Selexol plant (kJ <sub>el</sub> /kg <sub>CO2</sub> )	123.0
Ideal stages in the high pressure column	40	Steam consumption (net of Claus plant) (MJ/kg <sub>S</sub> )	6
Ideal stages in the low pressure column	60	CO <sub>2</sub> compression (kJ <sub>el</sub> /kg <sub>CO2</sub> )	222.6
High pressure column pressure losses (bar)	0.1		
Low pressure column pressure losses (bar)	0.1	<i>Syngas expander</i>	
Air purification section pressure losses (bar)	0.3	Pressure of delivered syngas (bar)	22
Main heat exchanger pressure losses (bar)	0.2	Polytropic efficiency (%)	88
Minimum ΔT in the main heat exchanger (°C)	2	Electrical/mechanical efficiency (%)	97
Minimum ΔT in the condenser/reboiler (°C)	2		
<i>OTM</i>		<i>Gas turbine and heat recovery steam cycle</i>	
Operating temperature (°C)	850	TIT (°C)	1350
O <sub>2</sub> selectivity (%)	100	Combustor pressure losses (%)	3
Pressure of feed air (bar)	19.75	Compressor polytropic efficiency	89.5
Sweep inlet temperature (°C)	750	Turbine stages maximum polytropic efficiency	89
Sweep inlet pressure (bar)	1.5	Pressure levels (bar)	145/23.5/2.5
Pressure losses on each membrane side (%)	5	Temperature SH/RH (°C)	540/540
Regenerative heat exchanger hot side exit temperature (°C)	600	Condensing pressure (bar)	0.042
Auxiliary combustor pressure losses (%)	3	HRSG gas side pressure loss (kPa)	3
Booster air compressor polytropic efficiency (%)	88	ΔT <sub>app</sub> /ΔT <sub>TH</sub> /ΔT <sub>SC</sub> (°C)	25/10/15
Compressor electrical/mechanical efficiency (%)	97	Electrical/mechanical efficiency (%)	98